*Semiconductor Physics, Quantum Electronics & Optoelectronics, 2017. V. 20, N 1. P. 79-84.*
doi: https://doi.org/10.15407/spqeo20.01.079

PACS 78.20.-e, 78.66.-w

# Determination of fundamental optical constants of $Zn_2SnO_4$ films

**A.O. Salohub[1], A.A. Voznyi[1], O.V. Klymov[2], N.V. Safryuk[3], D.I. Kurbatov[1], A.S. Opanasyuk[1]**
[1]*Sumy State University,*
*2, Rymskogo-Korsakova str., 40007 Sumy, Ukraine*
*E-mail: annkasalohub@gmail.com, opanasyuk_sumdu@ukr.net*
[2]*ISOM and Dpto. de* Ingeniería Electrónica
*Universidad Politecnica de Madrid, Ciudad Universitaria s/n, 28040 Madrid, Spain*
[3]*V. Lashkaryov Institute of Semiconductor Physics, NAS of Ukraine*
*41, prospect Nauky, 03680 Kyiv, Ukraine*

**Abstract.** Examined in this paper have been optical properties of polycrystalline films $Zn_2SnO_4$ deposited using the spray pyrolysis method within the range of substrate temperatures 250 °C to 450 °C in increments of 50 °C. The spectral dependences have been found for the following physical quantities: $k(\lambda)$, $n(\lambda)$, $\varepsilon_1(\lambda)$, $\varepsilon_2(\lambda)$ and defined as they change under the influence of substrate temperature $T_s$. Moreover, using the model by Wemple–DiDomenico it was calculated the dispersion energy $E_o$ and $E_d$ for this oxide. Two independent methods defined band gaps $Zn_2SnO_4$, which decreases from 4.21…4.22 eV down to 4.04…4.05 eV with increasing $T_s$ from 250 °C up to 450 °C.

**Keywords:** thin film, stannate zinc, spray pyrolysis, optical property, band gap, dispersion parameters.

Manuscript received 21.11.16; revised version received 23.01.17; accepted for publication 01.03.17; published online 05.04.17.

## 1. Introduction

In recent years, zinc stannate through its low cost, high optical transparency and low resistivity has been considered as alternative to the binary oxides (ITO, $SnO_2$, ZnO) and can have potential applications in a number of optoelectronic devices and solar energetics. In particular, ZTO thin films have found wide usage in photoelectrics. It should be emphasized that $Zn_2SnO_4$ consists of nontoxic and widespread elements in the earth's crust, which have the low cost of extraction [1]. Furthermore, the conductive contact with $SnO_2$ is replaced by more efficient zinc stannate, as a result, it allows increasing the energy conversion efficiency from 16.5 % up to 20.4 % in thin-film solar cells based on the heterojunction CdS/CdTe. Nowadays, all well-known photovoltaic devices with record parameters on the basis of the heterojunction necessarily have transparent front contact with ZTO [2]. The next step is to improve the performance of devices transparent oxide by way streamline the optical and electrical characteristics of the functional layers of the solar cell.

Today, for preparing ZTO thin films different methods are used: sputtering [3], chemical deposition from the gas phase [4], sol-gel [5], spray pyrolysis [6] *etc*. Among these techniques, the spray pyrolysis is an effective and inexpensive method for obtaining high-quality layers of oxides, due to operational simplicity, cost-efficiency, and the capability for large-scale production. A striking feature compared with the techniques given above is non-vacuum system of deposition. In the works [7-10] great attention is paid to studies of structural and physical properties of ZTO, and it is seen that significantly less studies are aimed at obtaining the zinc stannate by using spray pyrolysis [10-13]. It has been found that only in [11] the results of studying the optical properties of ZTO films are presented.

*Semiconductor Physics, Quantum Electronics & Optoelectronics, 2017. V. 20, N 1. P. 79-84.*
doi: https://doi.org/10.15407/spqeo20.01.079

It was this that played a key role in setting the goal of our work: first, to obtain thin films of $Zn_2SnO_4$ with high performances and, secondly, to investigate their structural and optical properties.

## 2. Materials and methods

ZTO films were deposited on glass substrates by using the spray pyrolysis in a laboratory setup that described in detail in [14]. The glass substrates were cleaned by ultrasound, then rinsed in distilled water and ethanol. Individually prepared precursor with of an aqueous solution of salts, pentahydrate tin tetrachloride (0.25 M) and the hexahydrate of zinc nitrate (0.5 M), also added a few drops of nitric acid to enhance solubility of salts. Herewith, the volume of this solution (6 ml), velocity of spraying the precursor (0.2 ml/min) and distance from spray nozzle to substrate surface (23 cm) were kept constant throughout all the experiment. Air was used as the carrier gas that supplied from the compressor under the pressure 0.2 MPa. The substrate temperature during deposition of the thin films were varied from $T_s$ = 250 °C up to 450 °C by the steps of 50 °C, and it was controlled using a thermocouple.

The structural properties of $Zn_2SnO_4$ were analyzed using X-ray diffraction. In particular, a Bruker D8 Avance A25 diffractometer equipped with a Lynxeye fast detector and employing copper Kα radiation in the θ–θ configuration were used to obtain diffraction patterns within the angle range 2θ from 10° to 90°, where 2θ is the Bragg angle. During the research, we used focused X-ray radiation in accord with the Bragg–Brentano scheme.

Optical studies of semiconductor films were carried out using spectrophotometer Solid Spec-3700 UV-VIS-NIR within the range of wavelengths λ = 250…1500 nm. As a result, it was measured the spectra of the reflection coefficient $R(\lambda)$ and transmittance $T(\lambda)$. In this case, with using the respective console, we reached double reflection of light from the surface of experimental samples, taking into account its reflection from the reference sample. Being based on the light reflection spectra $R(\lambda)$ in the region of low absorption of radiation, we calculated spectra of the refractive index $n(\lambda)$ and extinction $k(\lambda)$ for ZTO.

$$n = \frac{1+R}{1-R} + \sqrt{\frac{4R}{(1-R)^2} - k^2}, \qquad k = \frac{\alpha\lambda}{4\pi}. \tag{1}$$

Following the obtained above equation (1), from the values of the coefficients of refraction and extinction we determined the real $\varepsilon_1$ and imaginary $\varepsilon_2$ parts of the dielectric constant of the material using the according relationships [15, 16]:

$$\varepsilon_1 = n^2 - k^2, \ \varepsilon_2 = 2nk, \tag{2}$$

where $\varepsilon = \varepsilon_1 + \varepsilon_2 = (n+ik)^2$.

The dissipation factor [16] of the incident light was calculated using the following expression:

$$\tan\delta = \frac{\varepsilon_2}{\varepsilon_1}. \tag{3}$$

## 3. Results and discussion

### *3.1. Structural properties*

The data obtained in the previous studies indicated results of studying the surface morphology, chemical composition and some optical properties of ZTO films deposited using the spray pyrolysis were presented in [17]. Generally speaking, we examined a growth mechanism of the films and size of their grains in dependence on the substrate temperature. Using the method of X-ray spectral microanalysis (EDAX), we determined chemical composition of thin films, after that confirmed the presence of elements Zn, Sn and O in the films. Anyway, other doped components were not detected in the studied samples. Also, we evaluated the ratios of atomic concentrations $C_{Zn}/C_{Sn}$, $C_{Zn}/C_O$ and $C_{Zn+Sn}/C_O$ with increasing $T_s$ for ZTO.

Fig. 1 illustrates the diffraction patterns of ZTO thin films deposited at various temperatures. As we can see from the picture, in the patterns at 250 °C and 300 °C the lines at the angles 11.16…11.32° dominate. Also, there are less intense lines at the angles (16.20°, 22.51°…22.83°, 34.06°, and 46.15°). Nevertheless, nature of the peaks in diffractogram shows that the film of zinc stannate has a polycrystalline structure. Unfortunately, X-ray analysis was carried out partially. This is with account of disadvantage in the required number of diffraction lines for full analysis of the pattern of ZTO.

### *3.2. Optical properties*

Optical spectra for the coefficients of reflection $R(\lambda)$ and transmittance $T(\lambda)$ inherent to the studied samples are shown in Fig. 2. Preliminary results of these investigations were published in [17].

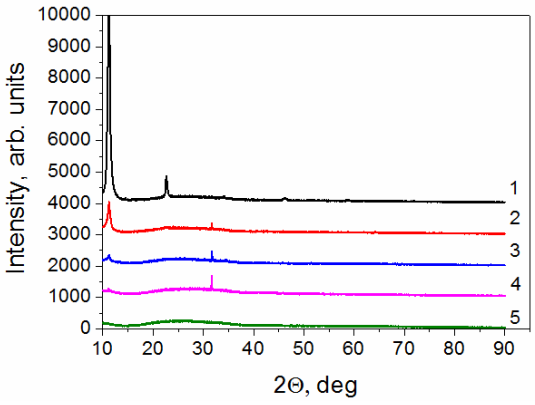


**Fig. 1.** X-ray diffraction pattern of the as-deposited ZTO films, where $T_s$, °C: 250 (*1*), 300 (*2*), 350 (*3*), 400 (*4*), 450 (*5*).

*Semiconductor Physics, Quantum Electronics & Optoelectronics, 2017. V. 20, N 1. P. 79-84.*
doi: https://doi.org/10.15407/spqeo20.01.079

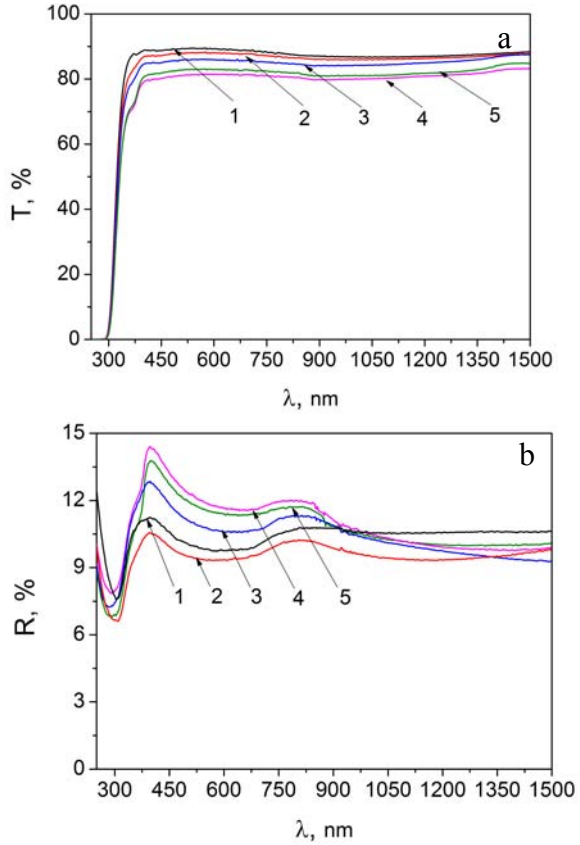


**Fig. 2.** Dependences for the coefficients of reflection (a) and transmittance (b) corresponding to ZTO thin films at $T_s$, °C: 250 (*1*), 300 (*2*), 350 (*3*), 400 (*4*), 450 (*5*).

By using the above mentioned results and expressions (1), we received values of the extinction coefficients $k$ and the refractive index $n$ for various λ, as illustrated by Fig. 3. As we can see from this figure, the extinction coefficient (Fig. 3a) decreases with increasing the wavelength, but this value increases with increasing the deposition temperature $T_s$. Thus, at the wavelengths $\lambda > 380$ nm, which correspond to the red boundary of the photoelectric effect, attenuation of the incident light is almost absent ($k \to 0$).

The dependence of the refractive index n against medium λ has falling in the wavelength range $\lambda = 400\ldots650$ nm (Fig. 3b). It is important to reiterate that this range corresponds to the region of low light absorption. Furthermore, when $\lambda = 400$ nm, the value of $n$ changes from 2.23 down to 1.96, which is in good agreement with the literature data [4] and [18].

Also, using the equation (2) we received the real $\varepsilon_1$ and imaginary $\varepsilon_2$ parts of the optical dielectric function for ZTO. Wavelength dependences for these parameters are given in Fig. 4. The obtained spectral distribution curves have a similar nature as for the previously described spectra of $k$ and $n$.

Note that the imaginary part of the dielectric function $\varepsilon_2$ of the material is 2-fold lower than the real part $\varepsilon_1$. In addition, at the wavelength $\lambda = 400$ nm the value of the real part of optical dielectric function lies within the range $\varepsilon_1 = 4.8\ldots3.8$, while that of the imaginary part lies within the interval $\varepsilon_2 = 0.019\ldots0.051$ ($\lambda = 290$ nm).

Respectively to the found values of $\varepsilon_1$ and $\varepsilon_2$, we plotted the dependence of the dissipation factor by using the equation (3). It can be seen from Fig. 5 that with increasing the frequency (energy of incident photons) the value of tan $\delta$ also increases. Moreover, the higher the substrate temperature, the greater the scattering coefficient.

Using the values of the absorption coefficients (that were determined and described in [17]) we plotted the spectral dependence of the coefficients of optical conductivity (σ) for the films of zinc stannate. The expression for σ has the following look [16]:

$$\sigma = \frac{\alpha n c}{4\pi}, \qquad (4)$$

where σ is the optical conductivity of thin films, α – absorption coefficient, $c$ – light velocity in vacuum.

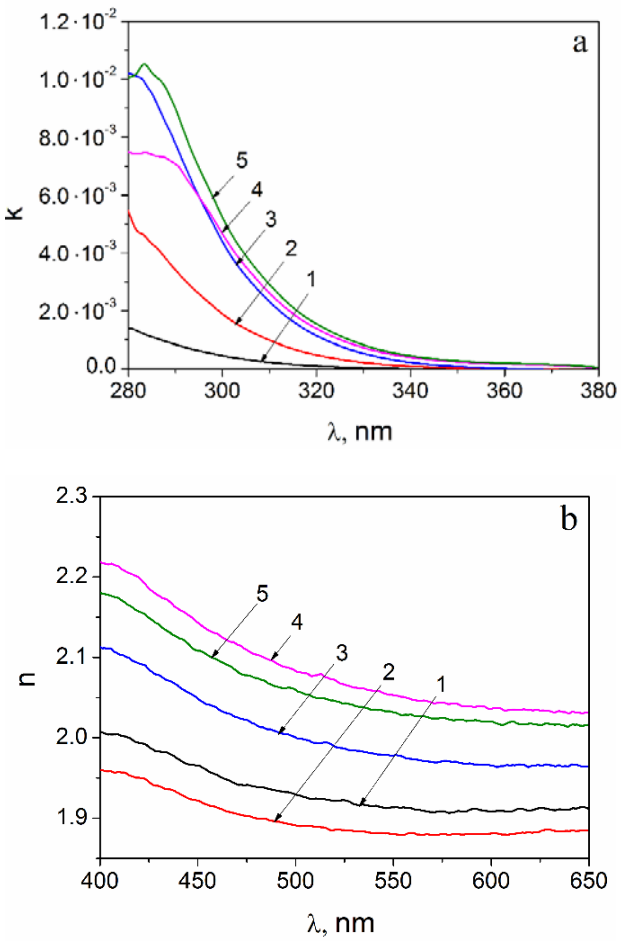


**Fig. 3.** Dependences of the coefficients of extinction $k$ (a) and refraction $n$ (b) for ZTO thin films at $T_s$, °C: 250 (*1*), 300 (*2*), 350 (*3*), 400 (*4*), 450 (*5*).

*Semiconductor Physics, Quantum Electronics & Optoelectronics, 2017. V. 20, N 1. P. 79-84.*
doi: https://doi.org/10.15407/spqeo20.01.079

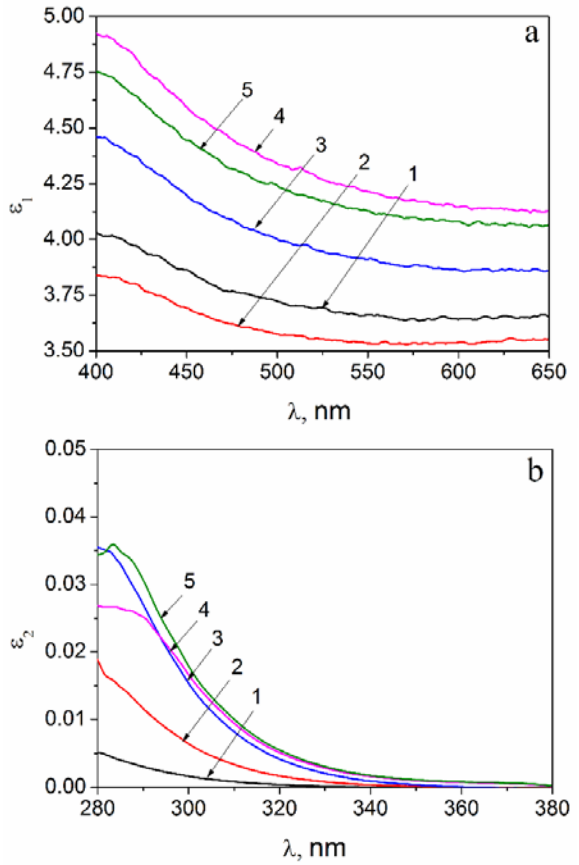


**Fig. 4.** Dependences of real $\varepsilon_1$ and imaginary $\varepsilon_2$ parts of the optical dielectric function corresponding to the ZTO thin films at $T_s$, °C: 250 (*1*), 300 (*2*), 350 (*3*), 400 (*4*), 450 (*5*).

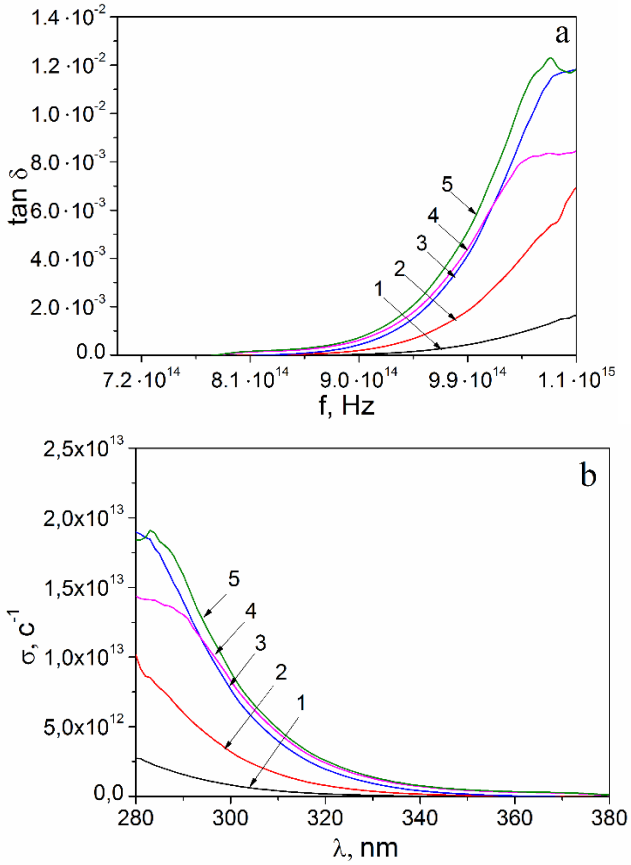


**Fig. 5.** Dependences of the dissipation factor (a) and optical conductivity (b) for ZTO thin films at $T_s$, °C: 250 (*1*), 300 (*2*), 350 (*3*), 400 (*4*), 450 (*5*).

These results are given in Fig. 5b. As it follows from the above relationships for the region of low light absorption, the values of σ decrease with increasing λ. Furthermore, it was discovered that the optical conductivity of ZTO thin films increases with increasing $T_s$, and the maximum value of this magnitude equals to $1.9 \cdot 10^{15}$ s$^{-1}$.

It is known [16] that the real part of the dielectric constant can be evaluated using the relation:

$$\varepsilon_1 = \varepsilon_\infty - B\lambda^2, \qquad (5)$$

where $B = \dfrac{e^2 N}{4\pi^2 c^2 \varepsilon_0 m^*}$, here $e$ is the electron charge, $N$ – free charge carrier concentration, $\varepsilon_\infty$ – high frequency dielectric constant, $\varepsilon_0$ – electrical constant of vacuum, $m^*$ – effective mass of the charge carrier.

Linearization of these dependences in the coordinates $\varepsilon_1 = n^2$ against $\lambda^2$ allows to find the value $\varepsilon_\infty$ by fitting a straight line with the $y$ axis, and the angle of slope to the $x$ axis values. The above equation for the parameter $B$ contains the ratio of the concentration of free charge carriers to the effective mass of charge carriers $N/m^*$ in the material. As a result, one can easy find the value of the parameter $B$.

According to Fig. 6, we obtained linear parts in the region $2.55 \cdot 10^5 < \lambda^2 < 4.25 \cdot 10^5$ nm$^2$. The straight line to $x$ axis formed some angle, which allowed us to determine the ratio $N/m^*$, and the point of crossing with the ordinate axis – values $\varepsilon_\infty$ (see Table).

The next step in interpretation of our results is application of the mathematical model of a harmonic oscillator [19]. With this model, one can determine optical dispersion parameters of these oscillators. It may be found from the relationship between the refractive index of the medium and the energy of harmonic oscillator:

$$n^2(h\nu) = 1 + \frac{E_d \cdot E_o}{E_o^2 - (h\nu)^2}, \qquad (6)$$

where $E_d$ is the dispersion energy that is a measure of the average strength of the interband optical transitions; $E_o$ – effective energy of single oscillator.

Using the relation (6), one can find the dispersion energy parameters of material $E_o$ and $E_d$. For this purpose, it was built the experimental dependence depicted in (Fig. 6). The value $(E_o E_d)^{-1}$ and angle of the $E_o/E_d$ were determined by extrapolation of linear parts.

The oscillator energy $E_o$ is related with average values of the optical band gap $E_g$ of the thin film, which is consistent with the model by Wemple–DiDomenico [19]. Therefore, using $E_o$ one can obtain the following value:

*Semiconductor Physics, Quantum Electronics & Optoelectronics, 2017. V. 20, N 1. P. 79-84.*
doi: https://doi.org/10.15407/spqeo20.01.079

$$E_g = \frac{E_o}{2}. \quad (7)$$

Summarizes in Table are the calculated energy parameters obtained for the zinc stannate. By using two independent methods, we determined the values of band gap for this material (dependences $(\alpha h\nu)^2$–$h\nu$ [17] and the model by Wemple–DiDomenico), which correlate well among themselves. It was ascertained that the dispersion energy of oscillators rapidly increased with growing the substrate temperature. However, the efficient dispersion energy decreases with increasing $T_s$.

**Table. Optical parameters for thin films ZTO.**

| $T_s$, °C | $N/m^*$, $m^{-3}$ | $\varepsilon_\infty$ | $E_o$, eV | $E_d$, eV | $E_g$, eV | $E_g^{opt}$, eV [17] |
|---|---|---|---|---|---|---|
| 250 | $2.45\cdot10^{37}$ | 3.65 | 8.44 | 22.08 | 4.22 | 4.21 |
| 300 | $9.93\cdot10^{36}$ | 3.54 | 8.39 | 20.58 | 4.19 | 4.18 |
| 350 | $6.03\cdot10^{37}$ | 3.86 | 8.23 | 24.56 | 4.11 | 4.15 |
| 400 | $1.27\cdot10^{38}$ | 4.13 | 8.13 | 27.18 | 4.06 | 4.05 |
| 450 | $8.94\cdot10^{37}$ | 4.06 | 8.12 | 26.01 | 4.05 | 4.04 |

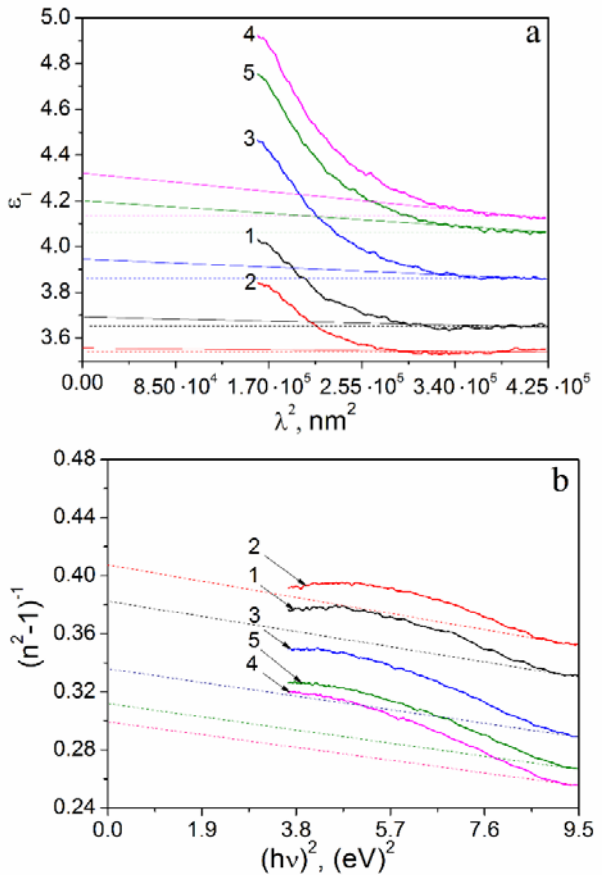


**Fig. 6.** Dependences of $\varepsilon_1$ against $\lambda^2$ (a) and $(n^2-1)^{-1}$ against $(h\nu)^2$ (b) for ZTO thin films at $T_s$, °C: 250 (*1*), 300 (*2*), 350 (*3*), 400 (*4*), 450 (*5*).

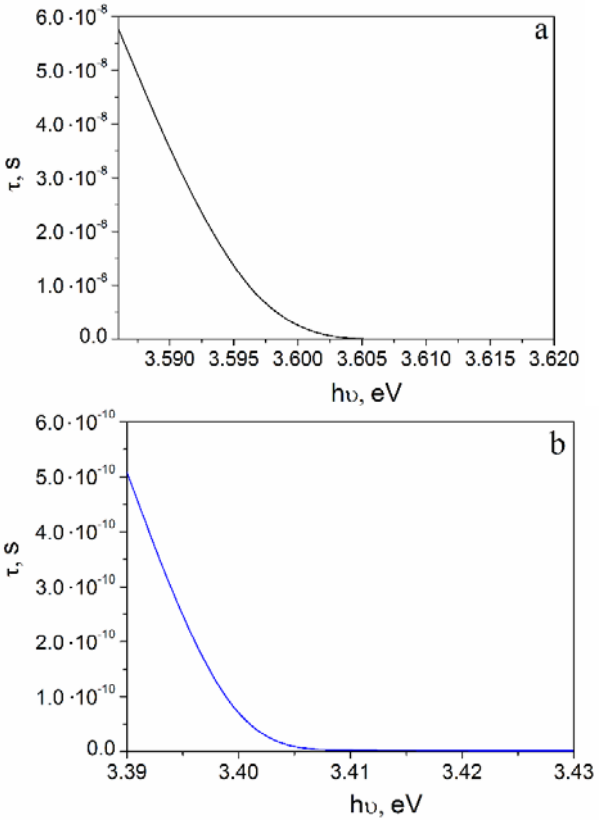


**Fig. 7.** Dependence τ versus $h\nu$ for ZTO thin film at $T_s$ = 250 °C (a) and 350°C (b).

The aforementioned calculations of the values $\varepsilon_\infty$ gave the opportunity to estimate the dielectric relaxation time of carriers in the material and to build its spectral dependence [16]:

$$\tau = \left|\frac{\varepsilon_\infty - \varepsilon_1}{\omega\varepsilon_2}\right|, \quad (8)$$

where ω is the cyclic frequency.

A typical dependence τ against the energy of incident light were obtained at temperatures $T_s$ = 250 °C and 350 °C as it is evident from Fig. 7. It is seen that the higher the substrate temperature, the lower the value of τ in the samples.

We can conclude, therefore, were first identified a different of optical material constants of ZTO films deposited by using spray pyrolysis. As a result, they can be used in development of a number of optoelectronic devices.

## 4. Conclusions

The optical properties of polycrystalline ZTO films deposited using spray pyrolysis. In addition, we plotted the following spectral dependences of the quantities: $k(\lambda)$, $n(\lambda)$, $\varepsilon_1(\lambda)$ and $\varepsilon_2(\lambda)$ for various temperatures of film deposition $T_s$. Using the model by Wemple–DiDomenico enabled to calculate dispersion energies $E_o$

and $E_d$ of this oxide. It is also worth noting that two independent methods allowed identification of the band gap for this material. It is reduced from 4.21…4.22 eV down to 4.04…4.05 eV at $T_s$ varying within the range 250…450 °C. Also, we have calculated the optical conductivity of this material at different wavelengths. It has been ascertained that the dielectric relaxation time of carriers in the films decreases with increasing $T_s$. Overall, we have investigated the fundamental optical parameters of ZTO films, which can be used in designing the devices of optoelectronics and solar energetics.

**Acknowledgement**

The work has been performed under the financial support of the Ministry of Education and Science of Ukraine (state registration numbers 0116U002619, 0115U000665c).

*References*

1. Minami T. Transparent conductive oxides for transparent electrode applications. *Semicond. Sci. Technol*. 2005. **20**, No. 4. P. 159-194.
2. Vijayalakshmi S. Investigations on ZnO:M (M = Al, Cd), $SnO_2$:Zn and $Zn_2SnO_4$ thin films deposited by spray pyrolysis method. http:// shodhganga.inflibnet.ac.in/handle/10603/26313.
3. Chen Y.C. and You H.M. Microstructures and dielectric properties of inverse-spinel structure $Zn_2SnO_4$ thin films by RF magnetron sputtering. *J. Mater. Sci.: Mater. Electron.* 2016. **27**, No. 2. P. 2031–2035.
4. Wang J.X., Xie S.S. and Gao Y. et al. Growth and characterization of axially periodic $Zn_2SnO_4$ (ZTO) nanostructures. *J. Cryst. Growth.* 2004. **267**, No. 1–2. P. 177–183.
5. Fu G., Chen H. and Chen Z. et al. Humidity sensitive characteristics of $Zn_2SnO_4$–$LiZnVO_4$ thick films prepared by the sol–gel method. *Sens. Actuators B.* 2002. **81**, No. 2. P. 308–312.
6. Kozhukharov S. and Tchaoushev S. Spray pyrolysis equipment for various applications. *J. Chem. Technol. Metall.* 2013. **48**, No. 1. P. 111–118.
7. Rozati S.M. and Shadmani E. Effect of Zn concentration on physical properties of nanostructure tin oxide films prepared by spray pyrolysis. *DIG J NANOMATER BIOS.* 2011. **6**. No. 2. P. 365–372.
8. Baruah S. and Dutta J. Zinc stannate nanostructures: hydrothermal synthesis. *Technol. Adv. Mater.* 2011. **12**, No. 1. P. 13004(1–18).
9. Wang J.X., Xie S.S. and Yuan H.J. et al. Synthesis, structure, and photoluminescence of $Zn_2SnO_4$ single-crystal nanobelts and nanorings. *Solid State Communs.* 2004. **131**, No. 7. P. 435–440.
10. Ganbavle V.V., Patil M.A. and Deshmukh H.P. et al. Pyrolysis development of $Zn_2SnO_4$ thin films deposited by spray pyrolysis method and their utility for $NO_2$ gas sensors at moderate operating temperature. *J. Anal. Appl. Pyrolysis.* 2014. **107**. P. 233–241.
11. Karthick A., Menaka S.M. and Uma G. et al. Structural and optical properties of $Zn_2SnO_4$ thin films prepared by spray pyrolysis. *J. Environ. Nanotechnol.* 2014. **3**, No. 3. P. 101–105.
12. Ardyanian M., Moeini M., and Juybari H.A. Thermoelectric and photoconductivity properties of zinc oxide – tin oxide binary systems prepared by spray pyrolysis. *Thin Solid Films.* 2014. **552**. P. 39–45.
13. Stambolova I., Konstantinov K. and Kovacheva D. et al. Spray pyrolysis preparation and humidity sensing characteristics of spinel zinc stannate thin films. *J. Solid State Chem.* 1997. **309**, No. 128. P. 305–309.
14. Dobrozhan O., Opanasyuk A.S. and Kurbatov D. et al. Influence of substrate temperature on the structural and optical properties of crystalline ZnO films obtained by pulsed spray pyrolysis. *Surf. Interface Anal*. 2015. **47**, No. 5. P. 601–606.
15. Starikov V.V., Ivashchenko M.M. and Opanasyuk A.S. et al. Surfase morphology and optical properties of CdSe films obtained by the close-spaced vacuum sublimation technique. *J. Nano-Electron. Phys.* 2009. **1**, No. 4. P. 119-126.
16. Abdel-Aziz M.M., Yahia I.S. and Wahab L.A. et al. Determination and analysis of dispersive optical constant of $TiO_2$ and $Ti_2O_3$ thin films. *Appl. Surf. Sci.* 2006. **252**, No. 23. P. 8163–8170.
17. Salohub A.O., Klimov O.V., Opanasyuk A.S. et al. Morphology, chemical composition and optical properties of $Zn_2SnO_4$ films obtained by pulsed spray pyrolysis. *Proc. NAP-2016 Intern. Conf.* 2016. **5**, No. 1. P. 01NTF23(1–5).
18. Satoh K., Kakehi Y. and Okamoto A. et al. Influence of oxygen flow ratio on properties of $Zn_2SnO_4$ thin films deposited by RF magnetron sputtering. *Jpn. J. Appl. Phys., Part 2.* 2005. **44**, No. 1–7. P. L34–L37.
19. DiDomenico M. and Wemple S.H. Oxygen-octahedra ferroelectrics. I. Theory of electro-optical and nonlinear optical effects. *Jpn. J. Appl. Phys.* 1969. **40**, No. 2. P. 720–734.